한국전산구조공학회
2005년 봄 학술발표회 논문집

일정체적 변단면 보의 정적 최적 단면

Static Optimal Shapes of Tapered Beams with Constant Volume

이 태 은* 강 희 종** 김 권 식** 이 병 구***
Tae Eun Lee Hee Jong Kang Kwon Sik Kim Byoung Koo Lee

Abstract

This paper deals with the static optimal shapes of simple beams which are subjected to a vertical point load. The area and second moment of inertia of the regular polygon cross-section of the tapered beams are determined, which have always same volume and same length for the parabolic taper. The differential equation governing the elastic curve is derived using the small deflection theory and solved numerically. By using the numerical results of deflections, rotations and bending stresses of such beams, the optimal shapes, namely, optimal section ratios, of the beams subjected to a single point load according to variation of load position parameters are determined and presented in the figures. Examples of the static optimal shapes for beams with a single load and multiple loads are reported. The design process of this study can be used directly for the minimum weight design of simple beams.

Keywords: *static optimal shape, simple beam, constant volume, regular polygon cross-section, tapered beam.*

1. Introduction

It is very important to determine the optimal structures from which the minimum structural behavior is arisen for given loading conditions. From this view point, the optimal shape of structures is very attractive reach subject in various engineering fields. Many investigators have been studied the optimal design for the structures [1,2,3,4,5].

In this study, the static optimal shapes of simple beams which are subjected to a vertical point load are determined. The objective tapered beams have always same volume and same length, whose cross-sectional depth is varied as the parabolic functional fashions. By using numerical results of deflections, rotations and bending stresses of such beams, the static optimal shapes are determined and its results are presented in the table and figures.

* Researcher, Institute of Construction Technology, Wonkwang University (Tel: 063-850-6718)
** Graduate Student, Department of Civil and Environmental Engineering, Wonkwang University
*** Professor, Department of Civil and Environmental Engineering, Wonkwang University

2. Objective Tapered Beam

Shown in Fig. 1(a) is a tapered beam with volume V and length l. The beams considered in this study always have the constant volume V and constant length l. The cross-sectional shape of the beam is the regular polygon cross-section, and its cross-sectional depth which is varied with the axial coordinate x is expressed as h. Consequently, the beam has the variable area and variable moment of inertia of area of cross-section expressed as A and I, respectively. The variation of depth h with x is defined in Fig. 1(b). Depths of the left end ($x = 0$) and mid-span ($x = l/2$) are h_0 and h_m, respectively. Here, a non-dimensional parameter defined as section ratio n is introduced as follows.

$$n = h_m / h_0 . \tag{1}$$

The cross-sectional properties A and I of the solid regular polygon cross-section with the integer m of side number and the cross-sectional depth h are given by, respectively,

$$A = c_1 h^2 , \tag{2}$$

$$I = c_2 h^4 , \tag{3}$$

where

$$c_1 = (m/2)\sin(2\pi / m) , \tag{4}$$

$$c_2 = (m/12)\sin(\pi / m)\cos^3(\pi / m)\{3 + \tan^2(\pi / m)\} , \tag{5}$$

in which the values of c_1 and c_2 with $m = \infty$, namely circular cross-section, are converged to π and $\pi / 4$, respectively. Also, it is noted that every centroidal axis of a regular polygon cross-section is a principal axis and has the same moment of inertia given in Eq. (3).

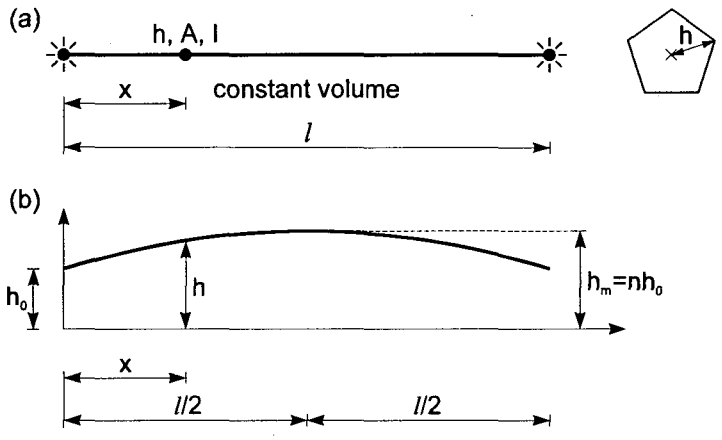

Fig. 1 (a) Tapered beam with regular polygon cross-section and (b) variation of cross-sectional depth

Now, define the variable cross-sectional depth h shown in Fig. 1(b). In this study, the parabolic, sinusoidal and linear tapers which are symmetric about mid-span are chosen as the variable depth h. For the parabolic taper which is chosen as a taper type in this study, the function of variable depth h through three points of $(0, h_0)$, $(l/2, nh_0)$ and (l, h_0) in rectangular coordinates (x, h) is determined as follows.

$$h = h_0\{-4c_3(x/l)^2 + 4c_3(x/l) + 1\},\ 0 \le x \le l. \tag{6}$$

where

$$c_3 = n - 1. \tag{7}$$

The volume V of parabolic taper can be calculated by using equations (2) and (4). The result is

$$V = \int_0^l A dx = (c_1 h_0^2 l)\beta \tag{8}$$

where the numerical factor β is

$$\beta = (1/15)(8n^2 + 4n + 3) \tag{9}$$

For another taper type such as the linear and sinusoidal tapers, the β value of respective taper can be obtained from similar method mentioned above.

3. Governing Equation

Shown in Fig. 2 is a deflected simple beam subjected to a vertical point load P in which the load position is depicted as l_p measured from the left end A. The elastic curve of beam is defined in the coordinates (x, y) where the origin is the left end A. At the typical material point (x, y), the rotation and bending moment are illustrated as θ and M, respectively. The end rotation at $x = 0$ is θ_a which is the unknown value to solve basically herein for determining the optimal shape of the beam.

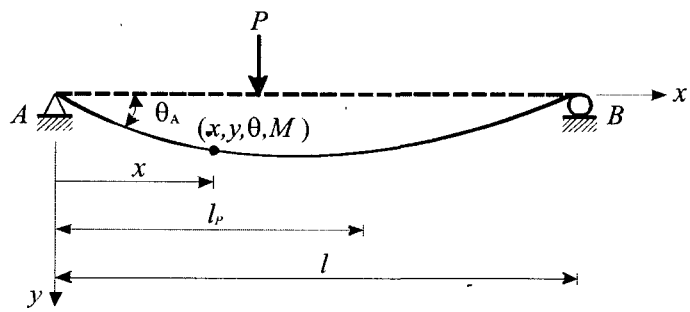

Fig. 2 Simple beam subjected to a vertical point load and its variables

The bending moment M at x can be obtained statically by using the equilibrium equations, or

$$M = (l - l_p)(P/l)x,\ 0 \le x \le l_p, \tag{10.1}$$

$$M = l_p(P/l)(l - x),\ l_p \le x \le l. \tag{10.2}$$

The well known differential equation that governs the elastic curve under the small deflection theory is

$$\frac{d^2y}{dx^2} = -\frac{M}{EI} \tag{11}$$

where E is Young's modulus.

Substituting Eqs. (3) and (10) into Eq. (11) gives the differential equations governing the elastic curve. The results are

$$\frac{d^2y}{dx^2} = -\frac{(l - l_p)(P/l)x}{Ec_2h^4},\ 0 \le x \le l_p, \tag{12.1}$$

$$\frac{d^2y}{dx^2} = -\frac{l_l(P/l)(l - x)}{Ec_2h^4},\ l_p \le x \le l. \tag{12.2}$$

The beam is simply supported so that the two boundary conditions at $x = 0$ and $x = l$ are obtained:

$$y = 0 \text{ at } x = 0, \tag{13}$$

$$y = 0 \text{ at } x = l. \tag{14}$$

which imply that the vertical deflections y are zero at both ends A and B.

The bending stress of extreme fiber σ_e in the cross-section due to M is calculated by the following equation.

$$\sigma_e = (M / I)h \tag{15}$$

To facilitate the numerical studies and to obtain the most general results for this class of problem, the following non-dimensional parameters are defined.

$$\xi = x/l \tag{16}$$

$$\eta = y/l \tag{17}$$

$$\alpha = l_p/l \tag{18}$$

$$p = \pi^2 Pl^4/(EV^2) \tag{19}$$

in which coordinates (x, y) and load poison l_p are normalized by beam length l as the non-dimensional coordinates (ξ, η) and load position parameter α, and p is the load parameter.

From Eqs. (16) and (17), the derivatives with respect to dx can be transferred into the derivatives with respect to $d\xi$ as follows.

$$\begin{aligned}\frac{dy}{dx} &= \frac{(1/l)dy}{(1/l)dx} = \frac{d(y/l)}{d(x/l)} \\ &= \frac{d\eta}{d\xi},\end{aligned} \tag{20.1}$$

$$\begin{aligned}\frac{d^2y}{dx^2} &= \frac{d}{dx}\left(\frac{dy}{dx}\right) = \frac{(1/l)d}{(1/l)dx}\left(\frac{d\eta}{d\xi}\right) \\ &= \frac{1}{l}\frac{d}{d(x/l)}\left(\frac{d\eta}{d\xi}\right) = \frac{1}{l}\frac{d}{d\xi}\left(\frac{d\eta}{d\xi}\right) \\ &= \frac{1}{l}\frac{d^2\eta}{d\xi^2}.\end{aligned} \tag{20.2}$$

Using Eq. (8) gives the cross-sectional depth h_0 at the end A ($x = 0$) as follows.

$$h_0 = \{V/(c_1\beta l)\}^{1/2} \tag{21}$$

Now, the non-dimensional differential equations are derived. Both Eq. (20.2) and function of variable depth h of Eq. (6) together with Eq. (21) are substituted into Eqs. (12.1) and (12.2) and the non-dimensional parameters of Eqs. (16)-(19) are used, or

$$\frac{d^2\eta}{d\xi^2} = -\frac{c_1{}^2\beta^2(1-\alpha)p\xi}{\pi^2 c_2\zeta^4},\ 0 \le \xi \le \alpha, \tag{22.1}$$

$$\frac{d^2\eta}{d\xi^2} = -\frac{c_1{}^2\beta^2\alpha\, p(1-\xi)}{\pi^2 c_2\zeta^4},\ \alpha \le \xi \le 1, \tag{22.2}$$

where

$$\zeta = -4c_3\xi^2 + 4c_3\xi + 1,\ 0 \le \xi \le 1, \tag{23}$$

Together with Eqs. (16) and (17), the two boundary conditions of Eqs. (13) and (14) become

$$\eta = 0 \text{ at } \xi = 0, \tag{24}$$

$$\eta = 0 \text{ at } \xi = 1. \tag{25}$$

In order to use the bending stress as one of the objective responses for obtaining the optimal shape of beam, the bending stresses of extreme fiber σ_e are normalized by E, V and l, or

$$\lambda = \frac{\sigma_e}{E}\left(\frac{l^3}{V}\right)^{1/2} = \frac{(c_1\beta)^{3/2}(1-\alpha)p\xi}{\pi^2 c_2 \zeta^3},\ 0 \le \xi \le \alpha, \tag{26.1}$$

$$\lambda = \frac{\sigma_e}{E}\left(\frac{l^3}{V}\right)^{1/2} = \frac{(c_1\beta)^{3/2}\alpha\, p(1-\xi)}{\pi^2 c_2 \zeta^3},\ \alpha \le \xi \le 1. \tag{26.2}$$

4. Numerical Methods

Based on the above analyses, algorithms were developed to determine the optimal section ratio n_{opt} for given beam. The optimal section ratio n_{opt} is defined as the section ratio under which the objective behavior of the beam is minimized so that the beam can endure most safely for the objective behavior. For determining n_{opt}, the differential equations have to be solved to obtain the static behaviors of the beam such as η, $\theta(=d\eta/d\xi)$ and λ at any coordinate ξ for a given set of beam parameters. The Runge-Kutta method[6] was used to integrate the differential equations and the Shooting method[6] was used to compute the unknown boundary condition, $d\eta/d\xi$ at $\xi = 0$. For solving the differential equation, the step size $\Delta\xi = 1/100$ in the Runge-Kutta scheme is used, under which the behavior values obtained herein are converged to four significant figures comparing the exact solutions of the uniform beams ($n = 1$).

By using the numerical data of beam behaviors which are obtained from solving the differential equations, n_{opt} is determined subsequently. The four kinds of objective behaviors of the beam such as ① $\eta_{\max}$, ② $\theta_{\max}$, ③ $\lambda_{\max}$ and ④ η_{ξ} (i.e. η at specified ξ) are chosen for determining n_{opt}. For example, the optimal section ratio n_{opt} for $\eta_{\max}$ is defined as the section ration n under which the maximum deflection $\eta_{\max}$ among η occurred along the axial coordinate ξ is minimized.

5. Numerical Examples and Discussion

First of all, Fig. 3 are presented, which show the determining process of optimal section ratio n_{opt} for a given set of beam parameters: integer side number $m = 3$ (regular triangle cross-section); position parameter $\alpha = 0.3$; and load parameter $p = 1$ (unit load). Note that the magnitude of p is not important since the superposition principle is effective in the theories developed in this study. The maximum responses such as $\eta_{\max}$, $\theta_{\max}$ and $\lambda_{\max}$ are presented according to varying the section ratio n in the range of $0 \le n \le 5$. For examples, the respective maximum response can be obtained as $\eta_{\max} = 0.0128$, $\theta_{\max} = 0.0618$ and $\lambda_{\max} = 0.1512$ for $n = 2$. See marks depicted ○ at the maximum points $n = 2$ in Fig. 3. Each maximum response decreases, reaches the lowest minimum one and increases as n is increased. It is clear that the each maximum value is minimized at n value of the lowest point, which now becomes to be the optimal section ratio n_{opt}. Consequently, the optimal section ratios n_{opt} with their minimized maximum behaviors for $m = 3$, $\alpha = 0.3$ and $p = 1$ are achieved at these lowest points. See the respective point marked ■ for ① $\eta_{\max}$; ▲ for ② $\theta_{\max}$; and ● for ③ $\lambda_{\max}$ in Fig. 3.

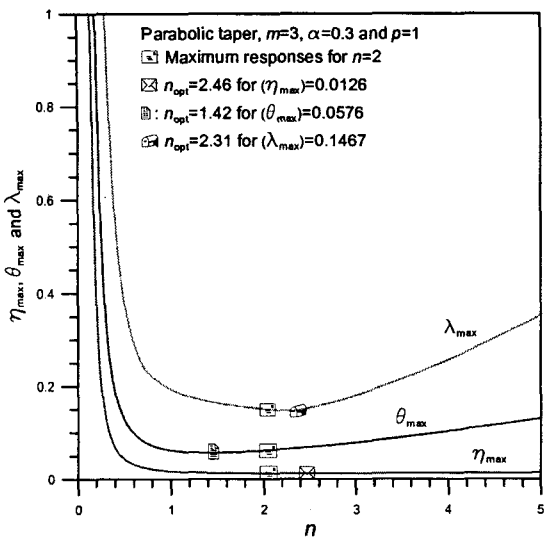

Fig. 3 Maximum responses versus n curves

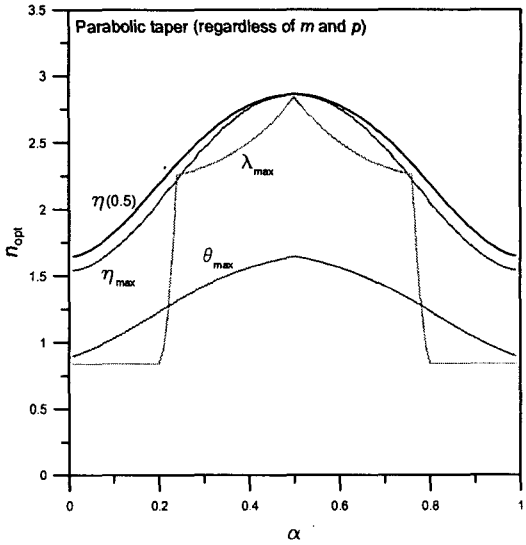

Fig. 4 n_{opt} versus α curves

In above numerical examples, n_{opt} is determined for only $m = 3$. Now, consider the effect the side number m on n_{opt} and their minimized response values. For $m = 3$, 4, 5 and ∞ (circular cross-section) with $\alpha = 0.3$ and $p = 1$, the values of n_{opt} and their minimized response values are calculated and summarized in Table 1. In this Table, n_{opt} for ④ $\eta_{\xi=0.5}$ is also calculated and presented. It is apparent that n_{opt} values for the selected objective behaviors are the same regardless of the side number m. For example, n_{opt} values for ① $\eta_{\max}$ are same as all $n_{opt} = 2.46$ regardless of m values. However, the minimized response values are different each other as m value is varied from 3 to ∞ as shown in Table 1. For the objective behaviors of deformations such as ① $\eta_{\max}$, ② $\theta_{\max}$ and ④ $\eta_{\xi=0.5}$, the minimized behavior value with smaller m gets smaller as the ratios shown in parentheses so that the regular triangular cross-section ($m = 3$) mostly advantages, while the circular one ($m = \infty$) disadvantages. The deformations cab be decreased about 21% only as if choosing $m = 3$ rather than $m = \infty$. However for bending stresses of ③ $\lambda_{\max}$, the advantage order is reversed. The circular cross-section ($m = \infty$) is the most advantage cross-section for minimizing the ③ $\lambda_{\max}$ in which the decreasing rate is about 29% comparing the value of $m = 3$.

Figure 4 shows n_{opt} versus α curves for the beam subjected to one point load at α which remains valid regardless of the side number m and load magnitude p due to the result of Table 1 and the superposition principle. It is natural that the curves are symmetric about $\alpha = 0.5$. Each n_{opt} value increases and reaches a peak at $\alpha = 0.5$, respectively, as α value is increased. Interestingly, the n_{opt} curves for ③ $\lambda_{\max}$ consist of six discontinuous independent curves. From theses figures, the minimum weight design of the simple beam for the respective behavior is possible when the beam is subjected to a vertical point load.

Table 1 n_{opt} and minimized object behavior for $\alpha = 0.3$ and $p = 1$ by m

Objective behavior	n_{opt}	Minimized value of objective behavior			
		$m = 3$	$m = 4$	$m = 5$	$m = \infty$ [1]
① η_{max}	2.46	0.0126(1.00) [2]	0.0145(1.15)	0.0150(1.19)	0.0152(1.21)
② θ_{max}	1.42	0.0576(1.00)	0.0665(1.15)	0.0685(1.19)	0.0697(1.21)
③ λ_{max}	2.31	0.1467(1.29)	0.1365(1.20)	0.1289(1.13)	0.1141(1.00)
④ $\eta(0.5)$	2.54	0.0123(1.00)	0.0141(1.15)	0.0146(1.19)	0.0149(1.21)

[1] Circular cross-section

[2] Figures in parentheses = Ratios against $m = 3$ or $m = \infty$.

6. Concluding Remarks

This paper deals with the static optimal shapes of simple beam which is subjected to a point loads. The area and second moment of inertia of the regular polygon cross-section of the tapered beams are determined, which have always same volume and same length for the parabolic taper. The differential equation governing the elastic curve is derived using the small deflection theory and solved numerically. By using the numerical results of deflections, rotations and bending stresses of such beams, the optimal shapes, namely, optimal section ratios, of the beams subjected to a single point load according to variation of load position parameters are determined and presented in the figures. Examples of the static optimal shapes for beams with a single load and multiple loads are reported. The design process of this study can be used directly for the minimum weight design of simple beams.

References

1. R.T. Haftka, Z. Grudal, Z. and M.P. Kamat, *Elements of Structural Optimization,* Kluwer Academic Publisher, 1990.
2. J.B. Keller, "The shape of the strongest column," *Archive for Rational Mechanics and Analysis,* Vol. 5, 1960, pp. 275-285.
3. E.F. Masur, "Optimal structural design under multiple eigenvalue constraints," *International Journal of Solids and Structures,* Vol. 20, 1984, pp. 211-2314.
4. S.J. Cox and M.I. Overton, "On the optimal design of columns against buckling," *SIAM Journal on Mathematical Analysis,* Vol. 23, 1992, pp. 287-325.
5. B.K. Lee and S.J. Oh, "Elastica and buckling load of simple tapered columns with constant volume," *International Journal of Solids and Structure,* Vol. 37, 2000, pp. 2507-2518.
6. B. Carnahan, H.A. Luther and J.O. Wilkes, *Applied Numerical Methods*, John Wiley and Sons, 1969.